Anti-VEGF Antibody Treatment of Glioblastoma Prolongs Survival But Results in Increased Vascular Cooption[1]

James L. Rubenstein*, Jin Kim[†], Tomoko Ozawa[‡], Michael Zhang[‡], Manfred Westphal[§], Dennis F. Deen[‡] and Marc A. Shuman*

*Division of Hematology/Oncology, University of California, San Francisco, San Francisco, CA; [†]Genentech, South San Francisco; [‡]Division of Neurological Surgery, Brain Tumor Research Center, University of California, San Francisco, San Francisco, CA and [§]Department of Neurological Surgery, University Hospital Eppendorf, Hamburg, Germany

Abstract

Vascular endothelial growth factor (VEGF) is an important mediator of the intense angiogenesis which is characteristic of glioblastoma. While genetic manipulation of VEGF/VEGF receptor expression has previously been shown to inhibit glioblastoma growth, to date, no study has examined the efficacy of pharmacologic blockade of VEGF activity as a means to inhibit intracranial growth of human glioblastoma. Using intraperitoneal administration of a neutralizing anti-VEGF antibody, we demonstrate that inhibition of VEGF significantly prolongs survival in athymic rats inoculated in the basal ganglia with G55 human glioblastoma cells. Systemic anti-VEGF inhibition causes decreased tumor vascularity as well as a marked increase in tumor cell apoptosis in intracranial tumors. Although intracranial glioblastoma tumors grow more slowly as a consequence of anti-VEGF treatment, the histologic pattern of growth suggests that these tumors adapt to inhibition of angiogenesis by increased infiltration and cooption of the host vasculature. *Neoplasia* (2000) **2,** 306–314.

Keywords: vascular endothelial growth factor, glioblastoma, angiogenesis, apoptosis, vascular cooption.

Introduction

During the past 40 years, there has been limited meaningful improvement in the prognosis for patients with glioblastoma; most malignant gliomas have proven to be refractory to conventional cytotoxic therapies [1]. Glioblastoma is the most common primary brain tumor and is among the most vascular of cancers [2]. Therefore, these tumors have appropriately been targeted for recent studies of angiogenesis and of anti-angiogenesis therapy [3].

Tumor growth is dependent upon blood supply. It is generally accepted that a tumor mass cannot exceed a diameter of 0.4 to 1.0 mm without establishing its own vasculature and that angiogenesis proceeds commensurate with the growth of the majority of malignancies [4].

Vascular endothelial growth factor (VEGF) has been implicated as a major paracrine mediator of glioma angiogenesis [5–13]. While a variety of peptide growth factors, such as basic fibroblast growth factor (bFGF), acidic fibroblast growth factor (aFGF), transforming growth factors alpha and beta (TGF-α, TGF-β), and hepatocyte growth factor (HGF), has been identified in malignant glioma specimens, levels of VEGF correlate best with microvessel density [9]. Moreover, the inhibition of VEGF/VEGF receptor interactions using neutralizing monoclonal antibodies, anti-sense and retroviral strategies has been shown to inhibit angiogenesis and growth of human glioblastoma cells in flank models of glioblastoma [8,10–12]. One study has also demonstrated the efficacy of *ex vivo* antisense inhibition of VEGF in the inhibition of angiogenesis and glioma growth in an orthotopic model [13].

Interactions between tumor cells and their normal microenvironment are critically important in the biology of cancer cells and have been shown to be associated with important regulatory events in gene expression in tumor cells [14]. For example, vitronectin, a major constituent of the extracellular matrix in malignant astrocytomas, has been shown to be produced by tumor xenografts specifically when implanted in the normal brain environment, not when grown in the subcutaneous compartment of the dorsal flank [15]. In addition, endothelial cells in different vascular beds express unique antigens and have distinct angiogenic properties [16]. To date, no study has determined the efficacy of pharmacologic inhibition of VEGF in the treatment of human glioblastoma tumors in an orthotopic environment. We have, therefore, performed an analysis on the outcome of systemic administration of a neutralizing antibody against human VEGF [17] in the treatment of intracranial glioblastoma cells stereotactically implanted in the striatum of adult athymic rats.

Materials and Methods

Glioblastoma Nude Rat Orthotopic Xenografts

Female homozygous nude rats, obtained from Harlan, Indianapolis, Indiana, weighed between 150- and 200 g. G55 glioblastoma cells [18] were grown to confluence, harvested and adjusted to a concentration of 200×10^6 cells/ml. Animals were anesthesized using ketamine/xylazine and their heads then immobilized in a stereotactic frame. Five microliters of cell suspension containing 1×10^6 cells was injected over 30 seconds into the right caudate nucleus using a Hamilton syringe with a blunt 25-gauge needle. Depth of injection from the bottom of the skull was 4 to 4.5 mm. Animals were weighed every other day and closely monitored at least twice daily both by the investigators and by the veterinary staff for signs of neurologic compromise. Animals exhibiting significant neurologic compromise, such as limping or any significant paresis which impaired ability to obtain food, were euthanized with sodium pentobarbital injection. All experiments involving the use of rodents were in accordance with protocols approved by the Animal Care and Use Committee of the University of California, San Francisco.

Anti-VEGF Antibody Treatment

After recovery from anesthesia, 12 animals were divided into two groups of six: control and anti-VEGF antibody. After receiving tumor implantation, animals were alternately assigned into the two groups. Stock anti-VEGF antibody was diluted in sterile PBS to a volume of 100 μl, which was injected using a 27-gauge needle into the peritoneal cavity. Injections were given every 48 hours, starting either on the day of tumor implantation or 7 days later.

Immunohistochemistry

Brains were removed from the cranial cavity and the right cerebral cortex and basal ganglia dissected as a block, embedded in OCT compound (Tissue Tek, Elkhart, IN) then frozen in liquid nitrogen. Sections 10 μm thick were prepared on a cryostat and stored frozen at -70°C. Later, sections were air-dried, fixed in acetone for 5 minutes (4°C), blocked in methanol/0.3% peroxide for 5 minutes, washed in PBS, then blocked in 10% normal goat serum for 30 minutes at room temperature. After incubation for 30 minutes with primary antibodies, the sections were washed in PBS, then treated with biotinylated secondary antibody for an additional 30 minutes. Subsequently, the sections were washed again in PBS then treated for 30 minutes with ABC reagent (Vectastain Elite Universal kit, Vector Laboratories, Burlingame, California) to create a peroxidase-conjugated avidin–biotin complex. Brown color was developed using 3,3-diaminobenzidine tablet sets followed by counterstain with Mayer's hematoxylin. Standard hematoxylin and eosin staining of brain sections was also carried out after the slides were fixed in 4% paraformaldehyde.

Integrin alpha V-beta 3 was stained with a polyclonal antibody from Chemicon (San Diego, California). VEGF was detected with a polyclonal antibody from Santa Cruz, Biotechnology (Santa Cruz, California). CD31 was detected with a monoclonal antibody from Pharmingen (San Diego, California).

TUNEL Staining

In situ end-labeling was performed using the in situ apoptosis detection kit from Boehringer Mannheim following the manufacturer's instructions. Levamisole, 2 mM, was included to suppress endogenous alkaline phosphatase activity. For quantitative histomorphometric analysis of apoptotic cells in situ, middle sections of tumors were imaged and captured at $\times2.5$ using a digital camera. Entire tumor areas were analyzed and quantified with the aid of a computer image analysis system. The sum total area of apoptotic cells was quantified and compared with total tumor area to calculate the apoptotic index. The means and SEM of the means were calculated for each tumor group. In all cases, TUNEL-positive cells correlated with cells whose nuclei appeared pyknotic under hematoxylin staining and light microscopy [19].

Vessel Density

We determined the mean vessel density per tumor by quantification of the relative area of CD31 immunoreactive structures per tumor by scoring two fields per tumor ($\times200$). Fields analyzed represented areas with the most intense angiogenesis detected per tumor. The mean vessel density per high-powered field and SEM of the mean were calculated for each tumor group [20].

Statistics

Statistical analyses for microvessel density, apoptotic index and image analysis used a Student's paired t-test. We used a log–rank test to determine significance in the survival analysis.

Results

Intracranial Glioblastoma Angiogenesis and Growth

For this study, we used G55 tumor cells which were derived from a human glioblastoma [18]. These cells have been shown to secrete VEGF constitutively in vitro [8]. Stereotactic implantation of 1×10^6 cells into the basal ganglia of nude rats resulted in the development of tumors in 100% of animals. Histopathologically, these tumors resemble glioblastoma in their hypervascularity and propensity for development of spontaneous necrosis. Moreover, tumor size increased rapidly over time resulting in increased intracranial pressure; by day 24 post-implantation, greater than 95% of these animals died or had to be sacrificed because of neurologic compromise secondary to increased intracranial pressure.

In characterizing the progression of angiogenesis with respect to tumor growth, we noted that vascular sprouts could be detected in groups of tumor cells surrounding the injection track as early as day 7 post-implantation, before the development of a solid tumor mass. These processes sometimes associated with larger capillaries exhibited
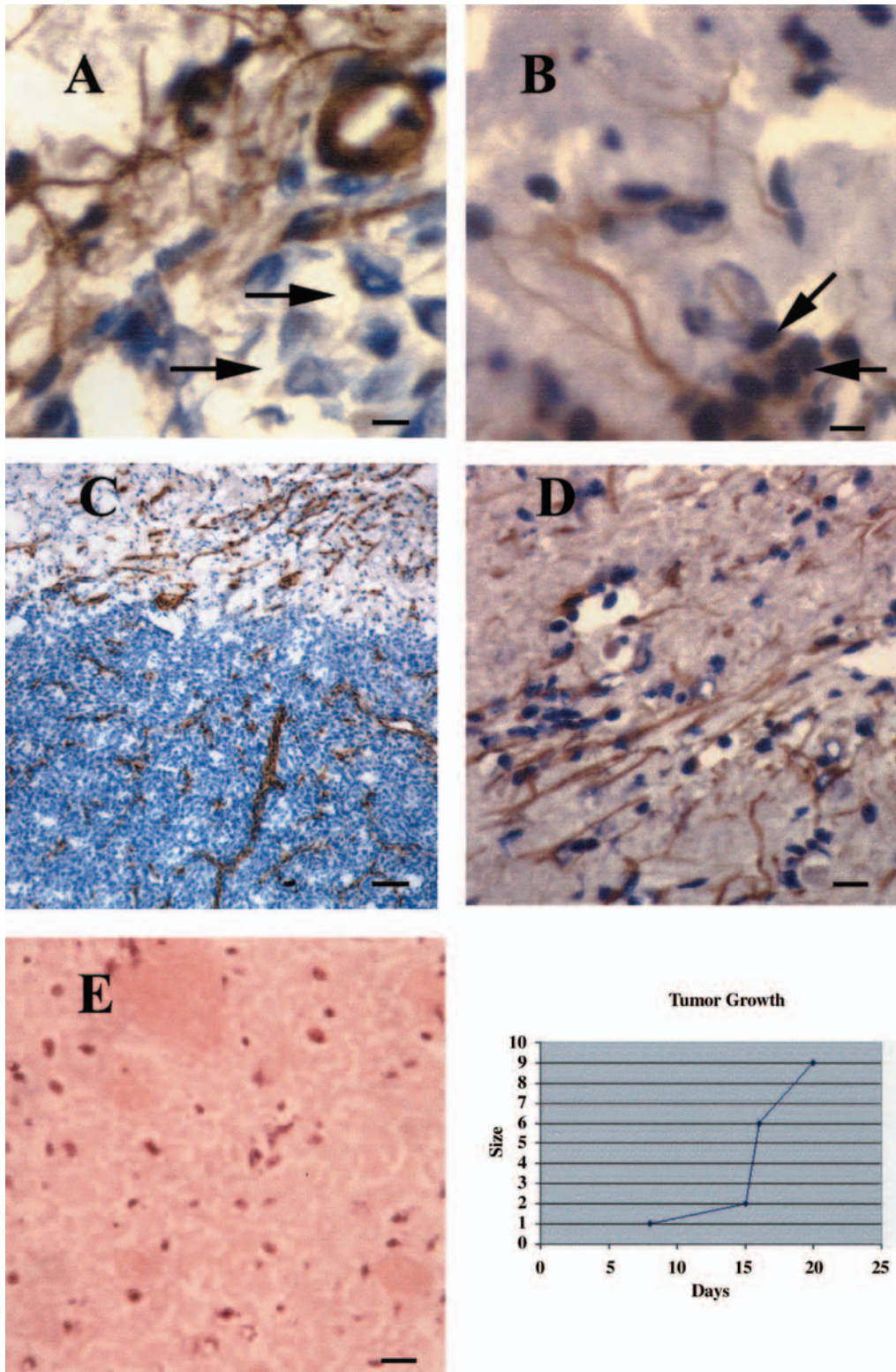
Figure 1. *(A) Individual glioma cells induce vascular process formation or sprouts 7 days post-tumor implantation. Vascular projections associated with a small capillary exhibit positive immunoreactivity for VEGF in close association with a group of tumor cells (counterstained with hematoxylin). In a parallel field (B), these projections also exhibit positive immunoreactivity for the angiogenic marker, integrin alpha V–beta 3, which was present on some individual tumor cells as well. Bar = 10 μm. At 12 days post-implantation (C), the tumors measure approximately 1 mm in maximum diameter and are already densely vascularized as evidenced by CD31 immunoreactivity. Bar = 60 μm. (D) A group of vessels in the tumor periphery appears to be growing in parallel, toward the tumor mass. These vessels also exhibited strong VEGF immunoreactivity. Bar = 30 μm. (E) There were no VEGF-immunoreactive vessels or cells in normal basal ganglia. Also, VEGF staining was blocked when a control peptide was added (not shown). (F) Graphic representation of G55 tumor growth after injection into the basal ganglia of athymic rats. Measurements represent maximum tumor diameter. By day 21, greater than 90% of the animals was sacrificed or succumbed to increased intracranial pressure. Growth curve determinations were repeated in three independent experiments with similar results.*

positive immunoreactivity both for VEGF (Figure 1*A*), as did some tumor cells (not shown), and for the integrin alpha V-beta 3 (Figure 1*B*), which is known to be induced in angiogenic vessels in brain tumors [21]. By day 12 post-implantation, the tumors were 1 mm in maximum diameter and were already densely vascularized as detected by CD31 immunoreactivity (Figure 1*C*). The periphery of these tumors exhibited intense neovascularization; new blood vessels appeared to grow linearly toward the tumor mass, and decreased in number and density in a gradient up to a distance of at least 4 mm into the cerebral cortex. These vessels also exhibited strong immunoreactivity for VEGF (Figure 1*D*), distinct from the vessels, neurons and glia of normal brain (Figure 1*E*).

These results suggest that secretion of VEGF by the tumor xenograft contributes to the rapid induction of blood vessel growth from surrounding normal brain and their chemotaxis to the tumor. In our experimental model, angiogenesis is detectable during the first week post-tumor implantation as individual glioblastoma cells appear to induce process formation from pre-existent vasculature. The earliest detectable solid tumor mass, 1 mm in diameter at day 12 post-implantation, is already highly vascularized.

Systemic Anti-VEGF Treatment Prolongs Survival

Next, we set out to determine the activity of a neutralizing antibody against human VEGF on the angiogenesis, growth and survival of intracranial human glioblastoma tumors using this model system. In each experiment, 12 animals with G55 tumor implantations were divided into two groups of six. Half of the animals received anti-VEGF by intraperitoneal injection (600 μg/every other day); half received an equivalent volume of PBS. The initial endpoint was survival. Institutional animal care guidelines were closely followed and animals that exhibited neurologic symptoms of weight loss in excess of 15% were euthanized to minimize suffering.

We reproducibly observed significant prolongation of animal survival in association with intraperitoneal anti-VEGF injection. Anti-VEGF treatment was most effective when initiated on day 1 (Figure 2). As expected, the median survival of the control animals was 18.5 days, the longest survived 20 days. The median survival of the anti-VEGF-treated animals was 34.5 days, a prolongation of 95% (P < .0001). Moreover, there was no toxicity associated with the treatment; in this experiment, animals in the anti-VEGF-treated cohort continued to maintain or gain weight at least 1 week beyond the median survival of the control group. The absence of toxicity is not surprising since the anti-VEGF antibody reacts against human but not rat VEGF.

When anti-angiogenesis therapy was initiated at day 7 after tumor implantation, median survival was significantly extended, but only by 25% (P < .05). These results are consistent with our observation that VEGF-associated angiogenesis begins during the first week, before the development of a solid tumor mass.
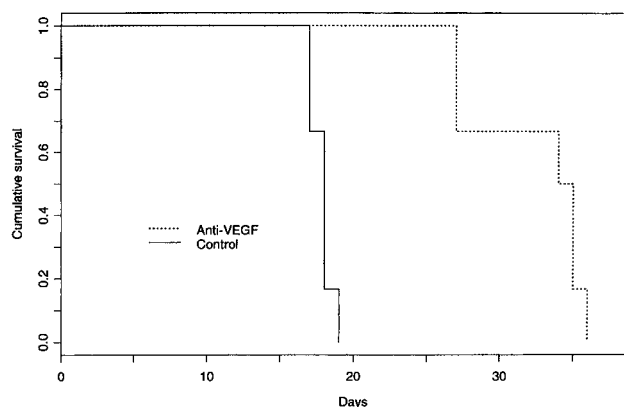
Figure 2. *Kaplan–Meier survival analysis of the outcome of athymic rats with intracranial human glioblastoma treated with anti-VEGF antibody. In this experiment, two groups of six rats received intraperitoneal injections of anti-VEGF antibody (600 μg/injection) or PBS every other day starting 2 hours after tumor implantation. The median survival in the control group was 18.5 days. The anti-VEGF-treated animals survived nearly twice as long, median survival 34.5 days (P < .0001). In four of four experiments, systemic anti-VEGF treatment was associated with survival prolongation in animals with intracranial glioblastoma.*

Inhibition of Angiogenesis and Induction of Apoptosis in Anti–VEGF-Treated Intracranial Tumors

At necropsy, tumors were analysed for vascularity and apoptotic index. Vascular density analysis using immuno-histochemical detection of the vascular antigen CD31 revealed a greater than four-fold reduction in vessel density within anti–VEGF-treated tumors in comparison to control (P < .001) (Figure 3). These results suggest that systemic anti-VEGF treatment inhibits glioma angiogenesis within the intracranial compartment and that in the conditions of this model, other angiogenesis factors, such as basic FGF, levels of which are elevated *in situ* in these tumors (not shown), are less important than VEGF, at least in the initial phase of brain tumor angiogenesis.

Vascularity and spontaneous necrosis are histologic cornerstones in the diagnosis of glioblastoma. Blockade of tumor angiogenesis has been shown to inhibit tumor growth by increasing the rate of tumor cell apoptosis, probably by multiple mechanisms including hypoxia, glucose deficiency and growth factor deprivation [19]. Apoptosis in control and anti–VEGF-treated tumors was quantified *in situ* by labelling fragmented DNA with the terminal deoxynucleotide transferase (TdT) labelling technique (TUNEL). The apoptotic index in control tumors was 1.9±0.65%. However, inhibition of VEGF activity was associated with a markedly higher apoptotic index of 31.2±10% (P < .01) (Figure 4). No TUNEL staining was detected when the enzyme terminal deoxynucleotidyl transferase was omitted from the reaction. In addition, there were no TUNEL-positive cells within the vascular endothelium or associated with normal neurons or glia in either the control or anti–VEGF-treated group.

Growth Delay and Satellite Tumor Formation in Anti–VEGF-Treated Tumors

G55 glioma xenografts normally grow as well-circumscribed masses within the rat basal ganglia, with borders
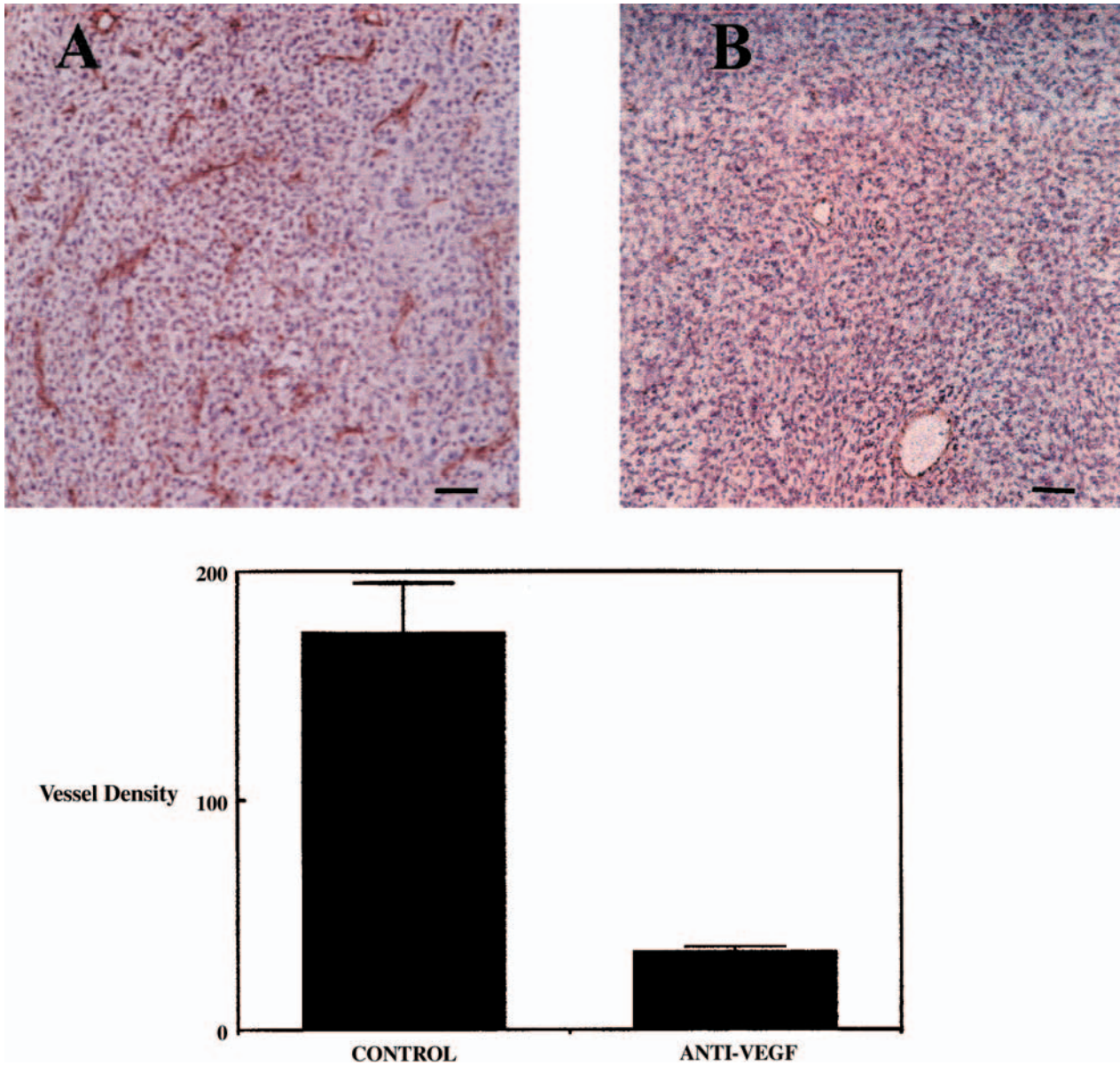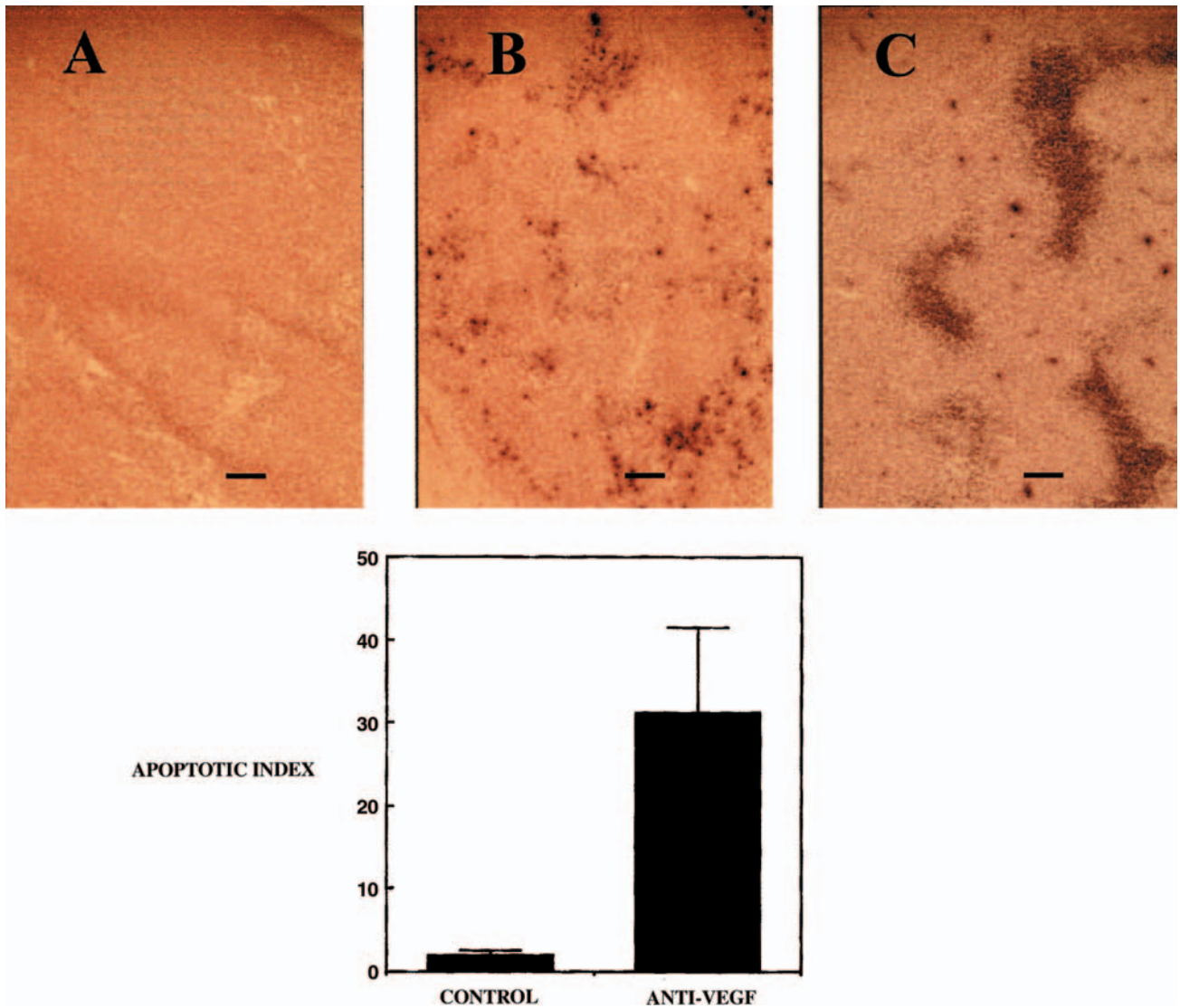
Figure 3. *(A and B) Systemic anti-VEGF treatment causes a marked reduction in the vascularity of intracranial human glioblastoma. There was a greater than four-fold reduction in vascular density as evidenced by CD31 immunoreactivity in glioblastoma tumors grown in animals treated with anti-VEGF (mean±SEM, n = 6 tumors/group) (P < .0001). Bar=60 μm.*

easily distinguished and dissected from normal rat brain. In animals treated with anti-VEGF, intracranial tumors adopted a more infiltrative pattern. We used computer-assisted digital image analysis to measure tumor area in the middle sections of control and anti-VEGF antibody-treated tumors. Histological analysis revealed that under normal conditions, these tumors grow as a single confluent mass with distinct borders (Figure 5A). We denoted the central tumor mass as the "primary tumor," which included any tumor mass in excess of 1 mm diameter (some animals in the anti−VEGF-treated cohort developed more than one tumor whose maximum dimension exceeded 1 mm; in these cases, the dimensions of the primary tumors were summed). In the anti-VEGF cohort, primary tumor masses were usually surrounded by multiple satellite tumors, ranging in size from

10 to 500 μm in diameter (Figure 5B). Many of these satellite tumors appeared to extend from the margin of the primary tumor, suggesting that these contain cells with increased invasive properties. In general, the size and number of the satellite tumors decreased with distance from the primary tumor (Figure 5C).

There was no significant difference in the total size of the primary tumors in the two groups (11.5 mm^2 vs. 13.2 mm^2; P > .557), despite the fact that the anti−VEGF-treated tumors analyzed survived on average 9.4 days longer than the control group (P < .0015) (Table 1). This result strongly suggests that anti-VEGF antibody treatment slowed but did not prevent primary tumor growth. Upon reaching an average threshold primary tumor size, 11 to 13 mm^2, the animals succumb to increased intracranial

Figure 4. *Systemic anti-VEGF treatment is associated with a marked increase in the incidence of TUNEL-positive cells in intracranial human glioblastoma. (A) There were no TUNEL-positive cells when the enzyme terminal deoxynucleotidyl transferase was omitted from the reaction mix. (B) The TUNEL assay demonstrated the presence of spontaneous apoptosis in control tumors. (C) There was a marked increase in apoptosis in tumors in animals treated with anti-VEGF antibody (mean±SEM, n = 9 tumors/group) (P < .011). Bar=60 μm.*
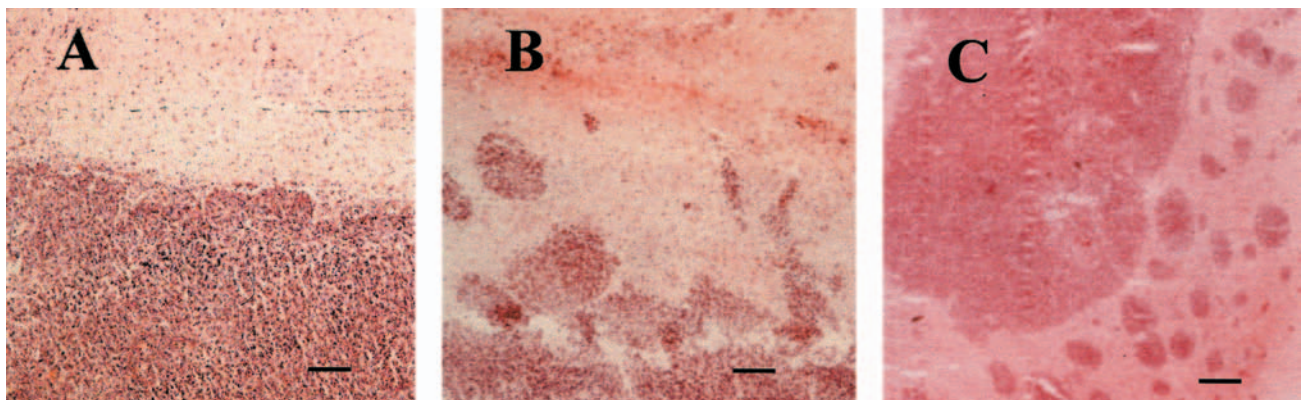
Figure 5. *Hematoxylin and eosin staining of control and anti–VEGF-treated tumors reveals that while control tumors (A) exhibit sharp tumor margins and grow as well-circumscribed non-invasive masses, the anti-VEGF antibody-treated tumors were markedly more heterogeneous with invasive-appearing borders (B) and exhibited a striking increase in the formation of satellite tumors (C). Satellites, composed of groups of tumor cells, approximately 5 to 50 in number and between 50 and 500 μm in diameter, were detected on the periphery of the primary tumor. Bar=80 μm (A and B); 120 μm (C).*

Table 1.

	Mean survival (days)	Mean primary tumor area (mm²)	Mean satellite tumor area (mm²)
Control (N=9)	18.7±1.3	11.5±1.5	0.097±0.07
Anti-VEGF (N=9)	28.2±2.1*	13.2±2.5**	2.24±0.7***

*P < .0015.
**P = .557.
***P < .008.

pressure. While the primary tumor sizes were the same in both cohorts, there was a 23-fold increase in satellite tumor area in the anti-VEGF antibody-treated animals compared with control animals (P < .008). In tumors from several anti–VEGF-treated animals, the area of the satellites approached or exceeded the area of the primary tumor. Taken together, these results suggest that the satellite tumors represent invasive islands of tumor cells which infiltrated normal brain. We found that greater than 90% of the satellite tumors was associated with at least one blood vessel as detected by CD31 and von Willebrand Factor (vWF) immunohistochemistry (Figure 6). Given that the extratumoral vessel density of the anti–VEGF-treated cohort was indistinguishable from that of normal brain, it is highly likely that these satellite tumors infiltrated the brain to adopt or "coopt" existing vessels in response to the consequences of anti-angiogenesis therapy. Thus, it is possible that metabolic deprivation and/or hypoxia serves as a stimulus for cells in the periphery of the tumor to become invasive and to migrate towards a gradient established by existing blood vessels.

Another difference between the primary tumor and the microsatellite tumors is that, unlike the primary tumors in which there was massive apoptosis particularly in the center of the tumor, no TUNEL-positive cells were detected in satellite tumors.

Discussion

This is the first study to examine the preclinical efficacy of pharmacologic inhibition of VEGF in an orthotopic model of glioblastoma. We demonstrate for the first time that systemic anti-VEGF therapy has the potential to significantly prolong survival in human glioblastoma. Our data suggest that systemic anti-angiogenesis therapy is not limited by the constraints of the blood–brain barrier; indeed, the very target for angiogenesis inhibition — the tumor neovasculature — is defective and leaky, lacking tight junctions and other specializations of the blood–brain barrier [22]. In addition, our data support the contention that VEGF production is critical in glioblastoma angiogenesis.

Our results also highlight several potential problems in the application of anti-angiogenesis therapy to brain tumors. To our knowledge, we have made the first observation that tumors may adapt to anti-angiogenesis therapy by increased invasiveness and cooption of host vessels. The formation of satellite tumors less than 0.5 mm in diameter, which appear to utilize existing blood vessels, may represent a general mechanism for resistance to anti-angiogenesis therapy. As we detected no TUNEL-positive cells in the satellite tumors, it appears that this is a successful adaptation.

While glioblastoma virtually never metastasizes out of the brain, it is one of the most infiltrative of all tumors, uniformly defying the most radical surgical resections. Our glioma model reflects this capacity and suggests that this invasiveness may be modulated in response to the tumor microenvironment. Because of the vascularity of the normal brain, and the well-developed vasculature of advanced glioblastomas, it is likely that the application of anti-angiogenesis strategies alone will not be successful in this disease. Our data suggest that anti-angiogenesis therapy for glioblastoma is most likely to be successful when initiated early after maximal tumor resection. Treatment of these tumors with a combination of anti-
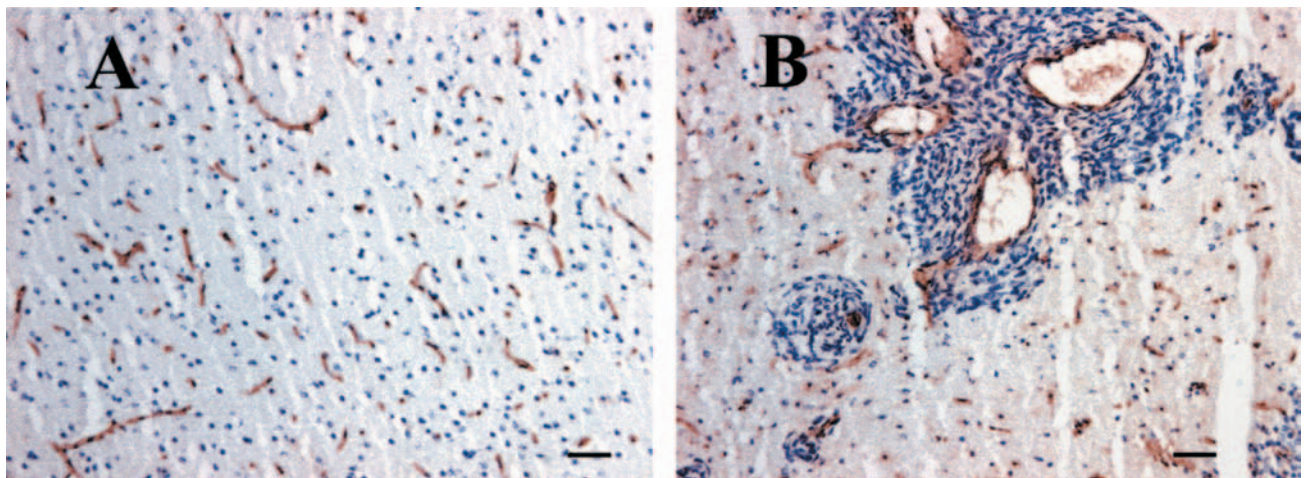
Figure 6. (A) Normal vascularity of rat basal ganglia as detected by CD31 immunohistochemistry (B). Greater than 90% of the satellite tumors associated with blood vessels, as evidenced by CD31 immunohistochemistry. Bar=60 μm.

angiogenesis agents and anti-invasive strategies to prevent tumor infiltration of the brain and association with its rich vasculature may prove to be a successful approach. As anti-angiogenesis therapies for a variety of types of tumors proceed in clinical trials, it may be valuable to determine whether increased invasiveness is a general mechanism by which tumors overcome strategies which target only the neovasculature.

It is worthwhile to note the similarities and differences between our results and those of other investigators. Chang *et al.* [13] demonstrated that the *ex vivo* anti-sense inhibition of VEGF production by U87 human glioblastoma cells causes a significant reduction in the size and vascularity of intracranial U87 tumors. The investigators compared tumor sizes at a similar time point post-implantation but did not compare the outcomes with respect to survival or the pattern of growth in the two cohorts.

Also, Holash *et al.* [23] reported a study on intracranial brain tumor angiogenesis using the rat RT-2 glioma cell line. In the rat glioma model system, angiogenesis occurs relatively late, at 28 days post-implantation, and is preceded by a period in which tumor cells appear to survive by association with the host vasculature, a process termed vessel cooption. Ultimately, the investigators detected apoptosis and regression of the host endothelium, resulting, first, in tumor necrosis and second, in a VEGF-associated angiogenic response. In our study using human glioblastoma cells, VEGF-associated angiogenesis begins much earlier, within 7 days post-implantation. Twelve-day-old tumors already exhibited a rich neovasculature. Increased vessel "cooption" appears to occur as a consequence of increased tumor invasion of normal brain. The latter is a consequence of angiogenesis inhibition. In our study, we did not detect apoptosis or regression of the vessels associated with satellite tumors. This process may occur more slowly in our model and therefore would not be detectable in a time frame that is limited by the progressive growth of the tumors.

It is tempting to speculate on the mechanism of satellite tumor formation. A variety of evidence suggests that these tumors exhibit increased invasive activity compared to the primary tumor. One possibility is that a threshold level of hypoxia induces the infiltrative phenotype, perhaps by increasing the expression of proteases such as the urokinase type plasminogen activator, as described [24]. Another possibility is that cells in tumor satellites exhibit a chemotactic response to factors in the extratumoral environment, such as gradients of oxygen, glucose, or growth factors produced by brain endothelia. Whatever the mechanism, this phenomenon must be taken into account when designing future therapeutic strategies.

References

[1] Hosli P, Sappino AP, DeTribolet N, and Dietrich PY (1998). Malignant glioma: should chemotherapy be overthrown by experimental treatments? *Ann Oncol* **9**, 589–600.

[2] Feigin I, Allen L, Lipkin L, and Gross SW (1958). The endothelial hyperplasia of the cerebral blood vessels with brain tumors and its sarcomatous transformation. *Cancer* **11**, 264–277.

[3] Fine HA, Figg WD, Jaeckle K, Wen PY, Kyritsis AP, Loeffler JS, Levin VA, Black PM, Kaplan R, Pluda JM, and Yung WKA (2000). Phase II trial of the anti–angiogenic agent thalidomide in patients with recurrent high-grade gliomas. *J Clin Oncol* **18** (4), 708–715.

[4] Hanahan D, and Folkman J (1996). Patterns and emerging mechanisms of the angiogenic switch during tumorigenesis. *Cell* **86**, 353–364.

[5] Takano S, Yoshii Y, Kondo S, Suzuki H, Maruno T, Shirai S, and Nose T (1996). Concentration of vascular endothelial growth factor in the serum and tumor tissue of brain tumor patients. *Cancer Res* **56**, 2185–2190.

[6] Berkman RA, Merrill MJ, Reinhold WC, Monacci WT, Saxena A, Clark WC, Robertson JT, Ali IU, and Oldfield EH (1993). Expression of the vascular permeability factor/vascular endothelial growth factor gene in central nervous system neoplasms. *J Clin Invest* **91**, 153–159.

[7] Plate KH, Breier G, Weich HA, and Risau W (1992). Vascular endothelial growth factor is a potential tumour angiogenesis factor in human gliomas *in vivo*. *Nature* **359**, 845–848.

[8] Kim KJ, Li B, Winer J, Armanin M, Gillet N, Phillips HS, and Ferrara N (1993). Inhibition of vascular endothelial growth factor-induced angiogenesis suppresses tumour growth *in vivo*. *Nature* **362**, 841–844.

[9] Samoto K, Ikezaki K, Ono M, Shono T, Kohno K, Kuwano M, and Fukui M (1995). Expression of vascular endothelial growth factor and its possible relation with neovascularization in human brain tumors. *Cancer Res* **55**, 1189–1193.

[10] Im S-A, Gomez-Manzano C, Fueyo J, Liu T-J, Ke LD, Kim J-S, Lee H-Y, Steck PA, Kyritsis AP, and Yung WKA (1999). Anti-angiogenesis treatment for gliomas: transfer of anti-sense vascular endothelial growth factor inhibits tumor growth *in vivo*. *Cancer Res* **59**, 895–900.

[11] Millauer B, Longhi MP, Plate KH, Shawver LK, Risau W, Ullrich A, and Strawn LM (1996). Dominant negative inhibition of Flk-1 suppresses the growth of many tumor types *in vivo*. *Cancer Res* **56**, 1615–1620.

[12] Saleh M, Stacker SA, and Wilks AF (1996). Inhibition of growth of C6 glioma cells *in vivo* by expression of antisense vascular endothelial growth factor sequence. *Cancer Res* **5**, 393–401.

[13] Cheng S-Y, Huang HJ, Nagane M, Ji XD, Wang D, Shih CC, Arap W, Huang CM, and Cavenee WK (1996). Suppression of glioblastoma angiogenicity and tumorigenicity by inhibition of endogenous expression of vascular endothelial growth factor. *Proc Natl Acad Sci USA* **93**, 8502–8507.

[14] Olumi AF, Dazin P, and Tlsty TD (1998). A novel coculture technique demonstrates that normal human prostatic fibroblasts contribute to tumor formation of LNCaP cells by retarding cell death. *Cancer Res* **58**, 4525–4530.

[15] Gladson CL, Wilcox JN, Sanders L, Gillespie GY, and Cheresh DA (1995). Cerebral microenvironment influences expression of the vitronectin gene in astrocytic tumors. *J Cell Sci* **108**, 947–996.

[16] Arap W, Pasqualini R, and Ruoslahti E (1998). Cancer treatment by targeted drug delivery to tumor vasculature in a mouse model. *Science* **279**, 377–380.

[17] Presta LG, Chen H, O'Connor SJ, Chisholm V, Meng YG, Krummen L, Winkler M, and Ferrara N (1997). Humanization of the anti-vascular endothelial growth factor monoclonal antibody for the therapy of solid tumors and other disorders. *Cancer Res* **57**, 4594–4599.

[18] Westphal M, Hansel M, Hamel W, Kunzmann R, and Holzel F (1994). Karyotype analyses of 20 human glioma cell lines. *Acta Neurochir* **126**, 17–26.

[19] Holmgren L, O'Reilly MS, and Folkman J (1995). Dormancy of micrometastases: balanced proliferation and apoptosis in the presence of angiogenesis suppression. *Nat Med* **1**, 149–153.

[20] Parengi S, O'Reilly MO, Christofori G, Holmgren L, Grosfeld J, Folkman J, and Hanahan D (1996). Anti–angiogenic therapy of transgenic mice

impairs *de novo* tumor growth. *Proc Natl Acad Sci USA* **93**, 2002–2007.

[21] Gladson CL (1996). Expression of integrin alpha V-beta 3 in small blood vessels of glioblastoma tumors. *J Neuropathol Exp Neurol* **55** (11), 1143–1149.

[22] Stewart PA, Hayakawa KA, Farrell CL, and Del Maestro RF (1987). Quantitative study of microvessel ultrastructure in human peritumoral brain tissue. *J Neurosurg* **67**, 697–705.

[23] Holash J, Maisonpierre PC, Compton D, Boland P, Alexander CR, Zagzag D, Yancopolous GD, and Wiegand SJ (1999). Vessel cooption, regression, and growth in tumors mediated by angiopoietins and VEGF. *Science* **284**, 1994–1998.

[24] Graham CH, Forsdike J, Fitzgerald CJ, and Macdonald-Goodfellow SM (1999). Hypoxia-mediated stimulation of carcinoma cell invasiveness via upregulation of urokinase receptor expression. *Int J Cancer* **80**, 617–623.